Ecological Modelling 368 (2018) 169–179

Contents lists available at ScienceDirect

Ecological Modelling

journal homepage: www.elsevier.com/locate/ecolmodel

The role of microzooplankton trophic interactions in modelling a suite of mesocosm ecosystems

Bei Su*, Markus Pahlow, A. E. Friederike Prowe

GEOMAR Helmholtz Centre for Ocean Research Kiel, Kiel, Germany

ARTICLE INFO

Article history:
Received 7 July 2017
Received in revised form
11 November 2017
Accepted 13 November 2017

Keywords:
Optimality-based plankton model
Trophic interactions
Feeding diversity
Dinoflagellates
Ciliates
Predator–prey size ratio

ABSTRACT

The zooplankton components in biogeochemical models drive top-down control of primary production and remineralisation, and thereby exert a strong impact on model performance. Who eats whom in oceanic plankton ecosystem models is often largely determined by body size. However, zooplankton of similar size can have different prey-size spectra. Thus, models with solely size-structured trophic interactions may not capture the full diversity of feeding interactions and miss important parts of zooplankton behavior.

We apply an optimality-based plankton ecosystem model to analyse trophic interactions in a suite of mesocosm experiments in the Peruvian upwelling region. Sensitivity analyses reveal a dominant role of trophic structure for model performance, which cannot be compensated by parameter optimisation. The single most important aspect governing model performance is the trophic linking between dinoflagellates and ciliates. Only with a bidirectional link, i.e., both groups can prey on each other, is the model able to reproduce the differential development of the microzooplankton communities in the mesocosms. Thus, we conclude that a solely size-based trophic structure may not be appropriate to represent the most important trophic interactions in plankton ecosystems. The diversity of feeding interactions needs to be adequately represented to capture community dynamics.

1. Introduction

Biogeochemical models usually incorporate plankton communities by means of NPZD-type formulations to represent major functional groups of plankton ecosystems, e.g., inorganic Nutrients, Phytoplankton, micro- and mesoZooplankton, and Detritus (Prowe et al., 2012a; Aumont et al., 2015; Le Quéré et al., 2016). While zooplankton and related parameters clearly exert a strong impact on model performance (e.g., Fulton et al., 2003a; Pahlow et al., 2008), finding and constraining the most appropriate representation of zooplankton dynamics remains a major challenge (Håkanson, 1995; Fulton et al., 2003b). Mesocosm experiments can help address this kind of questions as they allow frequent sampling of enclosed ecosystems, providing more coherent observations than is possible with field surveys and allowing for more natural conditions than laboratory studies.

In the present study, we examine the trophic roles of microzooplankton communities using data from two shipboard mesocosm experiments conducted in the coastal upwelling region off Peru (PU1, PU2, Hauss et al., 2012; Franz et al., 2012a,b). In this region, surface waters are characterised by high nutrient concentrations with low N:P ratios (compared to the Redfield N:P ratio of 16, Redfield, 1934) due to denitrification and anaerobic ammonium oxidation (anammox) in the underlying Oxygen Minimum Zone (OMZ, Deutsch et al., 2007; Kalvelage et al., 2013; Su et al., 2015). In order to investigate the influence of low N:P ratios on the growth and community composition of plankton, the mesocosms have been initialised with various DIN:DIP ratios. Distinctly different zooplankton communities developed in the PU1 and PU2 mesocosm experiments, with PU1 dominated by dinoflagellates and PU2 by ciliates, possibly related to the different nutritional quality of the phytoplankton communities (Franz et al., 2012b; Hauss et al., 2012).

Marine dinoflagellates can be autotrophic, heterotrophic or mixotrophic (Stoecker et al., 2017). Heterotrophic and mixotrophic species feed on a wide range of prey, including bacteria, phytoplankton, dinoflagellates and ciliates, using a variety of feeding strategies (Strom, 1991; Hansen, 1991; Jeong et al., 2010; Hansen et al., 2016). Several *Dinophysis* species feed on ciliates often larger than themselves (Hansen, 1991; Nishitani et al., 2008; Park et al., 2010). *Dinophysis caudata* accounted for up to 42% of the dinoflagellate community biomass in the PU1 and PU2 mesocosm

* Corresponding author.
E-mail address: bsu@geomar.de (B. Su).

https://doi.org/10.1016/j.ecolmodel.2017.11.013
0304-3800/

experiments (Hauss et al., 2012). Planktonic ciliates are another important component of the microzooplankton community in the ocean. They serve as food for larger organisms, e.g., copepods and fish larvae. Ciliates can consume a wide spectrum of food types and sizes (Yasindi and Taylor, 2006). Similarly to dinoflagellates, ciliates can also prey on bacteria, phytoplankton, dinoflagellates and ciliates (Sherr and Sherr, 1987; Dolan and Coats, 1991; Jakobsen et al., 1997; Jeong et al., 2013). Tintinnid ciliates are heterotrophic and feed primarily on photosynthetic algae and bacteria (Stoecker, 2012; Montagnes, 2013), whereas many oligotrich ciliates are mixotrophic (Dolan, 1992).

In plankton ecosystem modelling, trophic relations among zooplankton compartments are often based on body size (Hansen et al., 1994), which is generally considered a master trait for trophic interactions in plankton (Banas, 2011; Andersen et al., 2016). However, traits shaping feeding interactions are diverse and size relations between predators and prey can also result from foraging types and morphologies (Wirtz, 2012). Size ratios between predators and their prey are about 0.4–7 for dinoflagellates and 2.5–30 for ciliates (Hansen et al., 1994). Hence, dinoflagellates can prey on particles larger than their own size, whereas ciliates can only eat smaller prey (Jakobsen et al., 1997).

For analysing above mesocosm experiments, Marki and Pahlow (2016) developed an optimality-based model, which also forms the foundation for our present study. Optimality-based models rest on the assumption that evolution favours organisms with more efficient strategies in the continual competition for resources. In our present model, phytoplankton, dinoflagellates and ciliates are represented by optimality-based formulations (Pahlow and Prowe, 2010; Pahlow et al., 2013). These are mechanistically founded on trade-offs among energy and resource requirements of plankton organisms and can describe the observed behaviour of a wide range of phyto- and zooplankton species in laboratory experiments. A major advantage of these models is the low number of parameters required to describe fairly complex behaviour. For example, only six tuneable parameters need be calibrated for simulating four variables (C, N, P, Chl) with the phytoplankton model of Pahlow et al. (2013). Given the difficulties usually associated with constraining model parameters with (limited) observations (Schartau et al., 2017), keeping the number of parameters low greatly facilitates not only model calibration but also the disentangling of parameter and structural uncertainties.

Marki and Pahlow (2016) use their model to explore how microzooplankton respond to the different food quality of phytoplankton in terms of elemental composition, caused by the different nutrient enrichments in the mesocosms. Variations in phytoplankton C:N:P composition in response to ambient nutrient (DIN, DIP) stoichiometry in the Peruvian upwelling region alone, as described by the model of Pahlow et al. (2013), could not explain the differential development of the mesocosm plankton communities. Marki and Pahlow (2016) highlight the importance of intraguild predation and find that some of the differences among the mesocosms might be explained by variations in the zooplankton stoichiometry, pointing towards the importance of zooplankton flexible stoichiometry in marine ecological models. Marki and Pahlow (2016) also examine a more complex model configuration with two separate compartments for dinoflagellates and ciliates, with the larger (ciliates) feeding on the smaller (dinoflagellates) zooplankton, but this (size-based) modification did not improve model performance.

For the present study, we relax two restrictions applied by Marki and Pahlow (2016). (1) Instead of using pre-defined parameter sets for microzooplankton, we identify and optimise sensitive model parameters in order to separate parameter and structural model uncertainty. (2) We examine the effect of the size-based restriction that ciliates feed on dinoflagellates but not vice versa by introducing a new model configuration with a bidirectional link, i.e., dinoflagellates and ciliates can prey on each other. We base our analysis on the configuration with separate microzooplankton compartments for dinoflagellates and ciliates. This avoids a solely size-based trophic structure, and allows for a potentially greater diversity of trophic interactions. We then compare the predictive skill of the configurations with and without the bidirectional link in order to assess the importance of microzooplankton trophic interactions for plankton ecosystem modelling.

2. Methods

2.1. Data

We use data from two mesocosm experiments (PU1 and PU2, Table 1) in the upwelling region of the eastern tropical South Pacific off Peru (Hauss et al., 2012; Franz et al., 2012a,b). The influence of the stoichiometry of inorganic nutrient supply on growth and composition of plankton communities was investigated by monitoring mesocosms initialised with different nitrate and phosphate concentrations and ratios (Table 1). Each of PU1 and PU2 consisted of 12 mesocosms, with four replicates of three treatments (N:P ratios) in PU1 and three replicates of four treatments in PU2. Light intensity was reduced by 70% using shading nets, intending to mimic conditions at a depth of 10 m. All mesocosms were restocked with 5 μm-filtered ambient surface seawater on days 3 and 5 of the experiments, due to the large amounts of water required for sampling. Trace metal and silicate compounds were added to avoid trace metal and silicate limitation at the start of each experiment, and also on day 5 in PU2 only.

Samples were taken daily for measuring dissolved inorganic nutrients (DIN, DIP and SiO_3^{2-}), chlorophyll (Chl), particulate organic nitrogen (PON), particulate organic phosphorus (POP), and community composition (Hauss et al., 2012; Franz et al., 2012a,b). To measure dissolved inorganic nutrient concentrations, samples

Table 1
Summary of the mesocosm experiments PU1 and PU2 off Peru.

		PU1			PU2			
Latitude (S)		12°2.05′			16°0.01′			
Longitude (W)		77°47.33′			74°37.04′			
PAR (E m^{-2} d^{-1})		43.2			60.48			
Duration (days)		6			7			
Treatment N:P (mol mol^{-1})		20	3.4 (ambient)	2.8	16	8	5 (ambient)	2.5
DIN	(μmol L^{-1})	32	5.5	5.5	16.0	16.0	5.0	5.0
DIP	(μmol L^{-1})	1.6	1.6	2	1.0	2.0	1.0	2.0
Zooplankton community		Dinoflagellates dominant[a]			Ciliates dominant[a]			

[a] Hauss et al. (2012).

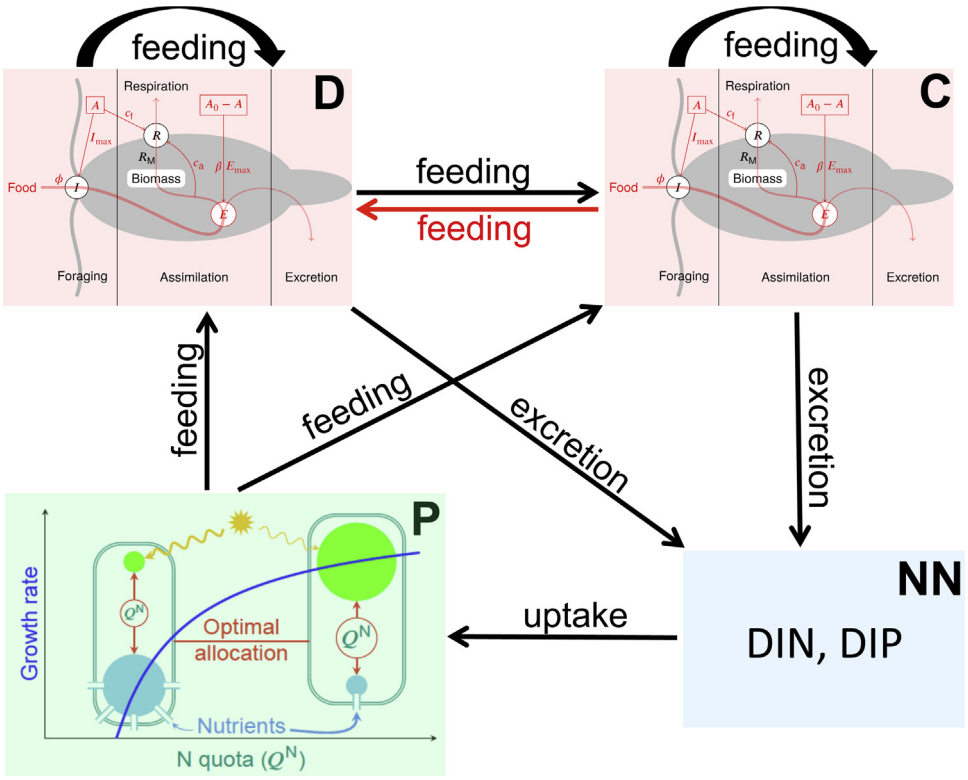

Fig. 1. Diagram of the optimality-based ecosystem model, which includes compartments (boxes) for nutrients (**NN**, DIN and DIP), phytoplankton (**P**), dinoflagellates (**D**) and ciliates (**C**). The phytoplankton is represented by the optimality-based chain model of Pahlow et al. (2013), and both dinoflagellates and ciliates are simulated by the optimal current-feeding model by Pahlow and Prowe (2010). The black arrows indicate all fluxes in the NNPDC configuration. The red feeding arrow indicates the additional flux for predation by dinoflagellates on ciliates in the NNPDrC configuration. (For interpretation of the references to colour in this figure legend, the reader is referred to the web version of the article.)

were filtered through 5 μm cellulose acetate filters and immediately analysed on board according to Hansen and Koroleff (1999) using a Hitachi U-2000 spectrophotometer. Chl concentration was measured using High Pressure Liquid Chromatography (HPLC) according to the modified method after Barlow et al. (1997). PON was measured with gas chromatography according to Sharp (1974) after filtration treatment. POP measurements were conducted with a modified method according to Hansen and Koroleff (1999) by incubating the defrosted filters in a household pressure cooker. Plankton community compositions were counted daily on board by counting Lugol-stained samples using an inverted microscope. To obtain plankton concentrations in biomass ($\mu g\,C\,L^{-1}$), the biovolume was calculated after approximation to geometric shapes (Hillebrand et al., 1999), and then converted to biomass with the carbon to volume relationships from Menden-Deuer and Lessard (2000).

2.2. Optimality-based NPZ model

Our optimality-based plankton ecosystem model comprises two inorganic nutrients (DIN and DIP), one phytoplankton compartment with variable C:N:P:Chl composition, and two zooplankton compartments, dinoflagellates and ciliates, representing the microzooplankton community (Fig. 1, see Eqs. (1)–(8) in Supplementary Material). The model equations are essentially the same as those in Marki and Pahlow (2016) and are provided in the supplementary material. As in Marki and Pahlow (2016), both dinoflagellates and ciliates feed on phytoplankton and both are intraguild predators, and ciliates also feed on dinoflagellates. We set up two model configurations (Fig. 1): (1) the NNPDC (two nutrients, NN, phytoplankton, P, dinoflagellates, D, ciliates, C) configuration, which corresponds to the NNPZZ-o model configuration in Marki and Pahlow (2016), and (2) the NNPDrC configuration, which introduces an additional trophic link, with dinoflagellates feeding also on ciliates. In contrast to Marki and Pahlow (2016), who used the pre-calibrated parameter sets from Pahlow and Prowe (2010) and Pahlow et al. (2013), we optimise the parameters of our model configurations to achieve the best model performance compared with the observations as described in Section 2.3, so that we can distinguish better between structural and parameter uncertainties.

The phytoplankton compartment is described by the optimality-based chain model (OCM) of Pahlow et al. (2013) (see Eqs. (9)–(16) in Supplementary Material). Briefly, the OCM is based on the concept that phytoplankton elemental composition results from optimally allocating cellular N and energy among competing requirements for nutrient (N, P) uptake, light-harvesting and growth (carbon fixation), so that the net growth rate is maximised. Requirements for N and P are defined via their physiological roles, i.e. P is essential for membranes and nucleic acids, and N is required for structural proteins and enzymes (Sterner and Elser, 2002). Since P is a major constituent of ribosomes, where proteins are synthesised, the model defines N and P colimitation as a chain of limitations, where P limits N assimilation and N limits all other biochemical processes (Ågren, 2004), i.e. nutrient acquisition and photosynthesis. Since the temperatures in the two experiments were very similar, the influence of temperature on phytoplankton growth is excluded from our analysis. However, we reduce the maximum rate parameter (V_0; Table 2) to account for the relatively low surface temperature in the upwelling region off Peru. The diurnal light cycle is included according to Brock (1981) to represent the light conditions in the mesocosms (Hauss et al., 2012; Franz et al., 2012a).

Zooplankton is described by an optimality-based model for zooplankton current feeding (OCF) developed by Pahlow and Prowe (2010) (see Eqs. (17)–(24) in Supplementary Material). The

Table 2
Model parameters for both NNPDC and NNPDrC configurations. Phytoplankton parameters are for the optimality-based chain model of Pahlow et al. (2013), and dinoflagellates and ciliates parameters are for the optimal current-feeding model of Pahlow and Prowe (2010) (Fig. 1).

Parameter	Description	Value	Units
Phytoplankton			
A_0	Potential nutrient affinity	*[a]	$m^3\ mol^{-1}\ d^{-1}$
α	Light affinity	*[a]	$m^2\ E^{-1}\ mol\ (g\ chl)^{-1}$
Q_0^N	Minimum N:C ratio	*[a]	$mol\ mol^{-1}$
Q_0^P	Minimum P:C ratio	*[a]	$mmol\ mol^{-1}$
V_0	Maximum rate parameter	4.0[c]	$mol\ mol^{-1}\ d^{-1}$
ζ^{Chl}	Cost of phytosynthesis coefficient	1.0[d]	$mol\ (g\ chl)^{-1}$
ζ^N	Cost of DIN uptake coefficient	0.6[b]	$mol\ mol^{-1}$
Dinoflagellates			
I_{max}^{Dino}	Maximum specific ingestion rate	*[a]	d^{-1}
ϕ_{Phy}^{Dino}	Prey capture coefficient for Phy	*[a]	$m^3\ mmol\ C^{-1}$
ϕ_{Dino}^{Dino}	Prey capture coefficient for Dino	*[a]	$m^3\ mmol\ C^{-1}$
ϕ_{Cil}^{Dino}	Prey capture coefficient for Cil	*[a]	$m^3\ mmol\ C^{-1}$
c_a^{Dino}	Cost of assimilation coefficient	0.33[e]	–
c_f^{Dino}	Cost of foraging activity coefficient	0.25[e]	–
Q_{Dino}^N	N:C ratio	0.20[f,g]	$mol\ N\ mol\ C^{-1}$
Q_{Dino}^P	P:C ratio	0.013[f,g]	$mol\ P\ mol\ C^{-1}$
R_M^{Dino}	Specific maintenance respiration	0.05[e]	d^{-1}
Ciliates			
I_{max}^{Cil}	Maximum specific ingestion rate	*[a]	d^{-1}
ϕ_{Phy}^{Cil}	Prey capture coefficient for Phy	*[a]	$m^3\ mmol\ C^{-1}$
ϕ_{Dino}^{Cil}	Prey capture coefficient for Dino	*[a]	$m^3\ mmol\ C^{-1}$
ϕ_{Cil}^{Cil}	Prey capture coefficient for Cil	*[a]	$m^3\ mmol\ C^{-1}$
c_a^{Cil}	Cost of assimilation coefficient	0.30[e]	–
c_f^{Cil}	Cost of foraging activity coefficient	0.30[e]	–
Q_{Cil}^N	N:C ratio	0.20[f,g]	$mol\ N\ mol\ C^{-1}$
Q_{Cil}^P	P:C ratio	0.013[f,g]	$mol\ P\ mol\ C^{-1}$
R_M^{Cil}	Specific maintenance respiration	0.05 [e]	d^{-1}

[a] Optimised parameters, see Table 3.
[b] Pahlow et al. (2013).
[c] Lower than in Pahlow et al. (2013) to account for the low temperature in the Peruvian upwelling region.
[d] Higher than in Pahlow et al. (2013) to better match observed phytoplankton concentration.
[e] Pahlow and Prowe (2010).
[f] Marki and Pahlow (2016).
[g] Assuming N:C higher than and N:P equal to Redfield proportions for zooplankton (Walve and Larsson, 1999; Kiørboe, 2013).

Table 3
Initial and calibrated parameter values. "Initial" are parameter values before calibration against observations. "Calibrated" are the parameter values after optimisation, and "Range" shows the spans of parameter values in Pahlow and Prowe (2010) and Pahlow et al. (2013).

Parameter	Initial	Calibrated		Range
		NNPDC	NNPDrC	
Phytoplankton				
A_0	0.15	0.216	0.474	0.06–1.0
α	0.9	1.24	0.943	0.5–3.7
Q_0^N	0.08	0.049	0.08	0.046–0.086
Q_0^P	2.0	0.801	1.84	0.8–2.7
Dinoflagellates				
I_{max}^{Dino}	2.9	2.01	2.06	2.9
ϕ_{Phy}^{Dino}	2.64	0.440	0.174	
ϕ_{Dino}^{Dino}	0.30	3.12	1.04	
ϕ_{Cil}^{Dino}	0/0.30	0	2.06	
Ciliates				
I_{max}^{Cil}	2.50	2.00	2.38	2.5–5.0
ϕ_{Phy}^{Cil}	0.24	0.661	0.765	
ϕ_{Dino}^{Cil}	0.12	0.323	3.12	
ϕ_{Cil}^{Cil}	0.06	1.28	0.918	

OCF optimises energy allocation between foraging activity and digestion, according to trade-offs among ingestion, assimilation efficiency, and respiration, to maximise net growth rate. The OCF assumes homeostasis, i.e. a constant C:N:P ratio and thus excretes or respires excess C, N, or P in inorganic forms when ingesting food with different C:N:P ratios. The two zooplankton functional groups (dinoflagellates and ciliates) are described by two different sets of parameters (Table 3). Temperature dependence is not considered for zooplankton, since the temperatures were similar in PU1 and PU2, and we optimise zooplankton parameters.

2.3. Model calibration and validation

In order to reduce the influence of parameter uncertainty on our conclusions regarding the effect of different model structures, we calibrate the model with the help of the fmincon function in MATLAB, which optimises parameter values by minimising the model-data discrepancies as quantified by a cost function. The fmincon function finds the minimum of a constrained nonlinear multivariate function and optimises all parameters simultaneously. We apply the 'interior-point' algorithm, which can handle large sparse as well as small dense problems. The algorithm satisfies bounds at all iterations, and can recover from NaN or Inf results (Byrd et al., 2010). The minimum change in variables for finite-difference gradients (DiffMinChange) and the step size factor for finite differences (FinDiffRelStep) are 0.01.

Our cost function is the root-mean-squared error (RMSE) normalised by the averages of the observed variables (Evans, 2003), which is defined as the coefficient of variation (CV) of the RMSE. We first calculate (CVs) for individual variables (CV_k) according to Eq. (1) and then obtain the actual cost function as the global average ($\overline{CV}$) according to Eq. (2):

$$CV_k = \sqrt{\frac{1}{T \times N}\sum_{j=1}^{T}\sum_{i=1}^{N}\left(\frac{M_{j,k} - O_{i,j,k}}{\overline{O}_{j,k}}\right)^2} \quad (1)$$

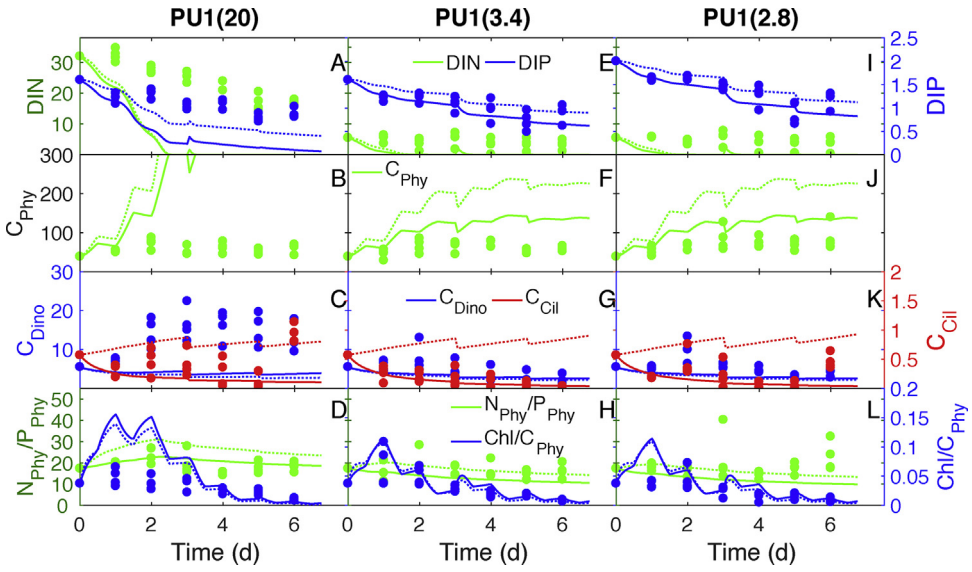

Fig. 2. PU1 data (disks) and model results for the NNPDC (dashed lines) and NNPDrC (solid lines) configurations. PU1(3.4) is the ambient treatment with DIN:DIP=3.4. PU1(20) and PU1(2.8) are the treatments with DIN:DIP=20 and 2.8, respectively. DIN and DIP are dissolved inorganic nitrogen and phosphorus concentrations in the mesocosms in μ mol L^{-1}. C_{Phy}, C_{Dino} and C_{Cil} are phytoplankton, dinoflagellate and ciliate concentrations in μ mol C L^{-1}. N_{Phy}/P_{Phy} is the phytoplankton cellular N:P ratio (mol mol^{-1}). Chl/C_{Phy} is the phytoplankton chlorophyll:carbon ratio (g chl $(mol\ c)^{-1}$).

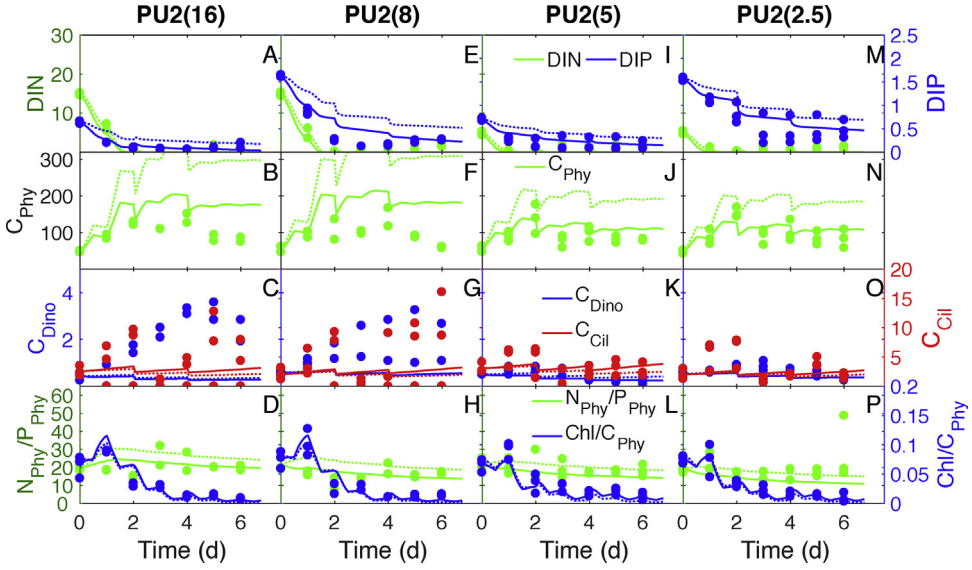

Fig. 3. Same as Fig. 2 but for PU2. PU2(5) is the ambient treatment with DIN:DIP=5. PU2(16), PU2(8) and PU2(2.5) are the treatments with DIN:DIP=16, 8 and 2.5, respectively.

$$\overline{CV} = \frac{1}{V}\sum_{k=1}^{V} CV_k \qquad (2)$$

where $M_{j,k}$ is the model value corresponding to observed data $O_{i,j,k}$, N is the number of replicates of each nutrient treatment, T is the number of sampling days. $T=7$ for both PU1 and PU2, and $N=4$ for PU1 and $N=3$ for PU2. V is the number of data types applied in the optimisation, which are DIN, DIP, phytoplankton (C_{Phy}), dinoflagellates (C_{Dino}), ciliates (C_{Cil}), and phytoplankton PON:POP and Chl:C ratios (N_{Phy}/P_{Phy} and Chl/C_{Phy}). $\overline{O}_{j,k}$, the mean of replicates within each treatment for every day, is used as a weight for each data type k to obtain dimensionless CV_k from data types with different units (Evans, 2003).

We use the cost function ($\overline{CV}$) first to decide which parameters to optimise during the data assimilation according to the sensitivity of $\overline{CV}$ to varying the parameters. Assuming that the plankton communities should be adapted to their environment, we then minimise $\overline{CV}$ with respect to the ambient treatments, i.e. N:P=3.4 for PU1 and N:P=5 for PU2 for our parameter optimisation.

The same parameter optimisation approach is applied to both the NNPDC and NNPDrC configurations, whence we compare the abilities of the two configurations to simulate the dynamics of the mesocosm experiments based on the optimised model results. To analyse the predictive capacity of the optimality-based ecosystem model for ecosystem dynamics, the performance of the calibrated model is then validated with the data for different nutrient treatments from the other mesocosms, i.e. those not used for calibration.

2.4. Sensitivity experiments

Since the additional trophic link in the NNPDrC configuration introduces another parameter and hence one degree of freedom, the NNPDrC(Phy) configuration is introduced to investigate the

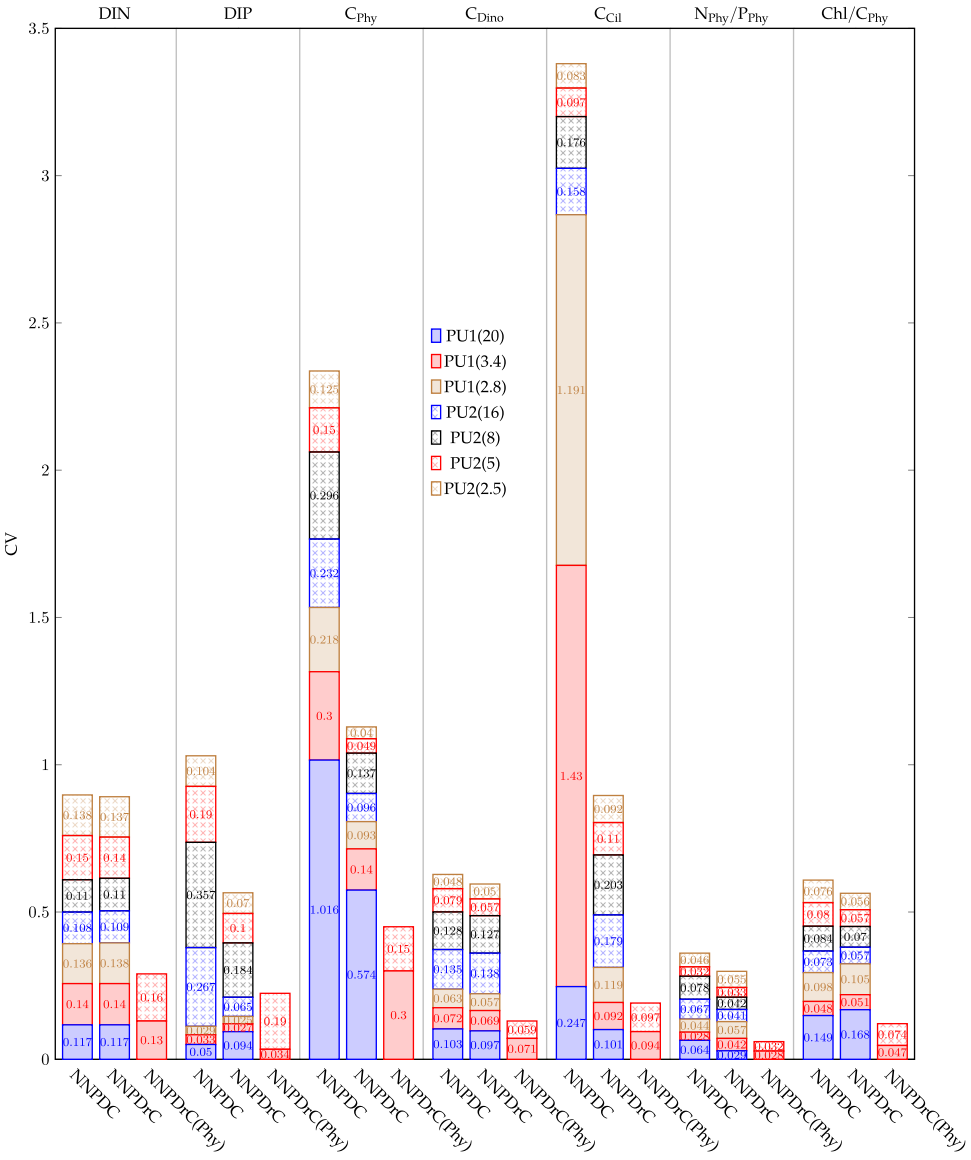

Fig. 4. CVs quantifying model-data discrepancies for the NNPDC, NNPDrC, and NNPDrC(Phy) configurations for each variable in all treatments. Flat-coloured bars show values for PU1, and cross-hatched bars are for PU2. The red bars are for the ambient treatments, i.e. PU1(3.4) and PU2(5). (For interpretation of the references to colour in this figure legend, the reader is referred to the web version of the article.)

influence of the degrees of freedom on the performance of the NNPDrC configuration. In NNPDrC(Phy), all phytoplankton parameters are fixed as calibrated for the NNPDC configuration and the zooplankton parameters are optimised as described in Section 2.3.

Marki and Pahlow (2016) suggest that microzooplankton respond to changes in food quality via variations in their phosphorus-to-carbon (P:C) ratio. In order to unravel the influence of microzooplankton stoichiometric plasticity on model performance, we analyse the sensitivity of our simulations to variations in the N:C and P:C ratios of microzooplankton (dinoflagellates and ciliates). The sensitivity experiments are conducted by reducing the microzooplankton P:C ratio from 0.013 to 0.0065, keeping the other parameters unchanged.

In order to elucidate the reasons why the model can not represent the high N:P treatments in PU1(20), sensitivity experiments are conducted by excluding the Chl:C ratio of phytoplankton from the cost function, attempting to allow the model to reproduce the remaining data. Parameters for only phytoplankton, dinoflagellates, ciliates, and both dinoflagellates and ciliates are tuned, respectively, in the PU1(Phy), PU1(Dino), PU1(Cil), and PU1(Zoo) experiments.

3. Results

The optimised parameters are mainly constrained within the ranges suggested in Pahlow and Prowe (2010) and Pahlow et al. (2013) and the final estimates are shown in Table 3. All other parameters are the same as in Pahlow and Prowe (2010) and Pahlow et al. (2013), except that V_0 is reduced to $4\,d^{-1}$ to represent the low temperature in the Peruvian upwelling region, and higher ζ^{Chl} to obtain a better match for phytoplankton concentration (Table 2). The optimised parameters indicate higher growth rates of phytoplankton and also higher predation of dinoflagellates on phytoplankton in NNPDC than in NNPDrC (Table 3). This can also be seen in Figs. 2 and 3, showing that phytoplankton concentrations are lower in NNPDrC, which is closer to the observations (Figs. 2B, F, J and 3B, F, J, N). Accordingly, CVs for phytoplankton in NNPDC are much larger than those in NNPDrC (Fig. 4).

The NNPDrC configuration fits the observations better than NNPDC in the ambient treatments (Figs. 2E–H and 3I–L). In PU1, after including dinoflagellates preying on ciliates, ciliate concentration decreases due to predation by dinoflagellates, matching the observations. Phytoplankton concentrations decrease in both

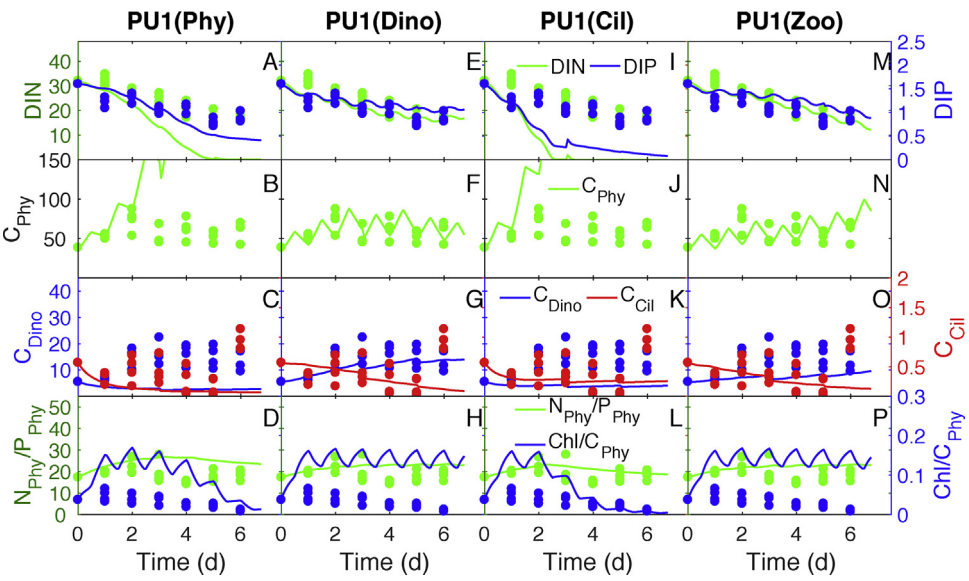

Fig. 5. Optimisation of different parameter subsets for the NNPDrC configuration for the PU1(20) experiment. Optimised parameters are A_0, α, Q_0^N and Q_0^P for PU1(Phy), I_{max}^{Dino} and ϕ_x^{Dino} for PU1(Dino), I_{max}^{Cil} and ϕ_x^{Cil} for PU1(Cil), and I_{max}^{Dino}, I_{max}^{Cil}, ϕ_x^{Dino} and ϕ_x^{Cil} for PU1(Zoo), $x \in$ [Phy, Dino, Cil], with all non-optimised parameters as in Table 2. Note that Chl/C_{Phy} is excluded from the cost function. All legends are the same as those in Fig. 2.

PU1(3.4) and PU2(5), which also represents the observations better (Fig. 4). The CVs for ciliate concentrations in NNPDC and NNPDrC are 1.53 and 0.20, respectively (red bars in Fig. 4). Thus, including predation by dinoflagellates on ciliates significantly improves model performance. CVs are reduced by 4.2%, 41.8%, 58.7% and 16.1%, respectively, for DIN, DIP, phytoplankton and dinoflagellate concentrations in NNPDrC compared with NNPDC. There is no significant improvement for Phytoplankon N:P and Chl:C ratios (red bars in Fig. 4).

For the NNPDrC(Phy) configuration, all phytoplankton parameters are fixed as calibrated for the NNPDC configuration and we optimise only the zooplankton parameters (Table 3). The NNPDrC(Phy) configuration still performs much better than NNPDC (Fig. 4). While the CVs for DIN, DIP, and phytoplankton of the NNPDrC(Phy) configuration are similar to those for NNPDC, the CVs for ciliates are very similar for NNPDrC and NNPDrC(Phy) (Fig. 4).

We analyse the ability of the optimality-based ecosystem model to simulate the mesocosm dynamics by applying the parameters calibrated for the ambient treatments to the mesocosms with different nutrient enrichments. Overall, NNPDrC fits the observations better than NNPDC, and the difference is much more pronounced in PU1 than in PU2 (Figs. 2, 3 and 4). The improvement in model performance is mostly due to the reduction in phytoplankton concentration in both PU1 and PU2, and the reduction in ciliate concentration in PU1. However, the NNPDrC configuration also fails to reproduce the observations in PU1(20), because it produces too high phytoplankton and too low nutrient concentrations (Fig. 2), which also results in high cost function values (Fig. 4).

Reducing the microzooplankton P:C ratio from 0.013 to 0.0065, as in Marki and Pahlow (2016), improves the model performance only slightly for the high N:P treatments (PU1(20) in Fig. A.1 and PU2(16) in Fig. A.2), where the dinoflagellates and ciliates increase only marginally in PU1 and PU2 respectively. Thus, variations in zooplankton stoichiometry do not appear to explain the discrepancies in the high N:P treatments.

The model can fit these data much better when tuning the parameters for only dinoflagellates or both dinoflagellates and ciliates (PU1(Dino) and PU1(Zoo), respectively, in Fig. 5). Nutrients, phytoplankton, microzooplankton, and phytoplankton N:P ratio in the mesocosms are all well represented, except that the increase in ciliate concentration at the end of the experiments can not be simulated (Fig. 5G and O). However, model performance does not improve when only the parameters for phytoplankton and ciliates are optimised (PU1(Phy) and PU1(Cil) in Fig. 5). Fig. 2 shows that the phytoplankton Chl:C ratio is too high for PU1(20) as long as DIN is available, i.e. until day 3. According to the behaviour of the OCM in Pahlow et al. (2013), it appears unlikely that our plankton model could reconcile the high DIN and DIP concentrations with the low phytoplankton Chl:C ratios observed throughout PU1(20). As expected, the Chl:C ratios of phytoplankton in PU1(Dino) and PU1(Zoo) are also higher than in the observations (Fig. 5H, P).

4. Discussion

With respect to the present study, the most important differences between the plankton communities in the PU1 and PU2 experiments are that dinoflagellates dominated the microzooplankton community in PU1, whereas ciliates dominated in PU2 (Table 1). The most abundant dinoflagellates in PU1 were the mixotrophic *Prorocentrum triestinium* and the heterotrophic *Dinophysis caudata*. Ciliates in PU2 included heterotrophic oligotrich ciliates and *Strombidium* sp.

The largest discrepancy between our model predictions and the observations for the PU1 and PU2 experiments occurs for ciliates in PU1 for the NNPDC configuration, as indicated by the CV (Fig. 4). Including the predation by dinoflagellates on ciliates in our NNPDrC configuration, brings ciliate concentrations significantly closer to the observations in PU1 (Fig. 2). This does not happen in PU2 (Fig. 3), where the CV of ciliates is already much lower than in PU1 for the NNPDC configuration. Owing to the large contribution of the ciliate CV in PU1 to the overall model-data discrepancy, the NNPDrC configuration thus performs significantly better than the NNPDC configuration.

The improved model performance could in principle be due to (1) a more realistic representation of trophic interactions, or (2) the slight increase in model complexity in the NNPDrC configuration resulting from the additional flux from ciliates to dinoflagellates, which requires an additional model parameter to be optimised. A first hint that allowing for dinoflagellates preying on ciliates indeed adds realism to the model is found in the microscopic observations:

Dinophysis caudata, which can prey on morphologically larger ciliates (Hansen, 1991; Nishitani et al., 2008; Kim et al., 2012), was abundant in PU1, but not in PU2 (Hauss et al., 2012).

Another indication is obtained from the performance of the NNPDrC(Phy) configuration, which uses the same phytoplankton parameters as NNPDC. Hence, the NNPDrC(Phy) configuration has less degrees of freedom than NNPDC, yet performs much better (Fig. 4). The performance of DIN, DIP, and phytoplankton remains similar to NNPDC, but is much better for ciliates. Therefore, we conclude that the improved performance of the NNPDrC configuration is indeed due to a more realistic representation of trophic interactions, which indicates that the diversity of feeding interactions needs to be adequately represented to capture community dynamics.

The NNPDrC configuration represents the ecological dynamics better than NNPDC for all mesocosms (Fig. 4), including those with different nutrient supply ratios. Nevertheless, performance is worse for higher N:P enrichment ratios, especially for N:P=20 in PU1 (Figs. 2, 3 and 4). A possible explanation for the failure to reproduce the data for N:P=20 in PU1 may be the lack of representation of mixotrophs in the model (Flynn et al., 2013; Stoecker et al., 2017). In fact, several mixotrophic dinoflagellate species occurred in both PU1 and PU2 (Hauss et al., 2012), which may not be represented adequately by the separate phytoplankton and zooplankton compartments in our model (Flynn et al., 2013; Larsen et al., 2015). Mixotrophy is increasingly seen as a widespread trophic strategy for protist plankton with implications not only for our understanding of community ecology but also for the biological pump and ocean change (Flynn et al., 2013; Mitra et al., 2014b). However, few dynamic ecosystem models to date explicitly include mixotrophs (e.g. Flynn and Mitra, 2009; Ward et al., 2011). In order to account for the various types of mixotrophic strategies, new model structures for PFT-type models (Mitra et al., 2016) as well as for size-based models (Chakraborty et al., 2017) are being put forward.

Marki and Pahlow (2016) hypothesised that microzooplankton respond to changes in food quality in terms of N:C ratios, rather than N:P ratios, by varying their P:C ratios. With their more simplified model configuration, Marki and Pahlow (2016) highlight the importance of microzooplankton stoichiometric plasticity in response to changes in elemental composition of their food, e.g., that the P:C ratio of microzooplankton could decrease with increasing N:P in the food. When decreasing the microzooplankton P:C ratio in NNPDrC, the model reproduces the observations slightly better (Figs. A.1 and A.2), especially in mesocosms with high N:P ratios (N:P=20 in PU1). However, this improvement is much smaller than that by optimising all dinoflagellate parameters (Fig. 5), which indicates that effects of microzooplankton stoichiometric plasticity may be easily obscured by uncertainties in other model parameters.

Disregarding the Chl:C_{Phy} ratio, we can mostly reproduce the N:P=20 treatment of PU1 by optimising only zooplankton parameters (Fig. 5M–O). However, the impossibility to match simultaneously Chl:C_{Phy} and C_{Phy} indicates that the model does this for the wrong reasons: The model predicts much higher phytoplankton Chl:C ratios than observed (Fig. 5P), hence phytoplankton growth rates are likely too high, which is compensated by strong grazing as also reflected in the rather high estimates for $I_{\max}^{Dino} = 6\,d^{-1}$ and $\phi_{Phy}^{Dino} = 0.52\,m^3\ mmolC^{-1}$ here (cf. Table 3).

The failure of our model to reproduce the high N:P treatment indicates a certain rigidity of the model behaviour, probably related to the low number of parameters (Franks, 2009). However, we consider this failure an important aspect of the model as it clearly indicates a deficiency, either in the model (in the form of missing processes) or in the experimental setup (in the form of unintentional resource limitation). Phytoplankton growth may have been hampered in mesocosms with N:P=20, preventing utilisation of all available DIN and DIP. Several trace metals including iron have been added in sufficient quantities to prevent limitation by them (H. Hauss, pers. comm.). Nevertheless, the most likely explanation might still be that the large amount of DIN added in this treatment could have induced limitation by some other trace element, which might explain the high left-over concentration of DIN in these mesocosms. At this point, this argument remains somewhat speculative, but it may be an attractive hypothesis for reconciling the N:P=20 treatment with the other treatments. Furthermore, this mismatch points to the importance of including trace metal limitation in our model in future work.

Our model study together with the work of Marki and Pahlow (2016) demonstrates how plankton ecosystem models can be employed to unravel how plankton community dynamics respond to changing environmental or ecological conditions, which are difficult to quantify in the mesocosm studies themselves. Several other mesocosm studies have been analysed in a similar manner (Thingstad et al., 2007; Wirtz, 2013; Larsen et al., 2015). Larsen et al. (2015) used the *minimum microbial food web* (MMFW) model of Thingstad et al. (2007) to interpret plankton dynamics in three mesocosm studies differing in nutrient and mesozooplankton predator manipulations. In parallel to our study, Larsen et al. (2015) needed an additional trophic link (ciliates eating diatoms) to reconcile the MMFW with observations. However, while this modification of the MMFW was specific for one mesocosm treatment, the bidirectional link in our optimality-based model improves model performance for all treatments in the PU1 and PU2 experiments (Fig. 4).

Our bidirectional trophic link between dinoflagellates and ciliates can be viewed as an important element of intraguild predation within the microzooplankton community, which has been estimated to account for as much as 79% of microzooplankton production being recycled within the microzooplankton, thus dominating over mesozooplankton predation (Franzé and Modigh, 2013). Very few biogeochemical models explicitly consider intraguild predation within the zooplankton (e.g., Ward et al., 2014). In particular, models describing trophic interactions based solely on body or cell size (Banas, 2011; Acevedo-Trejos et al., 2016) may miss these trophic links entirely.

In addition to mixotrophy and intraguild predation, other issues currently hinder a more realistic representation of zooplankton in ecosystem models. The computational demand of global biogeochemical models strongly restricts the complexity of their ecosystem components (Fulton et al., 2003b), where zooplankton communities are usually represented by just one or very few functional groups (Mitra et al., 2014a). More complex representations of plankton communities remain restricted to local models (D'Alelio et al., 2016) or coarse resolution models with relatively short time scales (Follows et al., 2007). The zooplankton compartments strongly influence model dynamics, e.g., in terms of stability (Cropp et al., 2017) or coexistence (Cropp and Norbury, 2012; Prowe et al., 2012b; Vallina et al., 2014), but the parameterisation of zooplankton behaviour is fraught with a high degree of uncertainty (Fulton et al., 2003a; Sailley et al., 2013). Together with the long-standing dichotomy between complexity and explanatory power and the need for upscaling the behaviour of few known species to represent entire communities, plankton modelling has reached a critical stage asking for new ways to capture community dynamics. Our optimality-based formulation may help reduce the uncertainty with respect to the representation of zooplankton behaviour, as it can reproduce observed feeding behaviour (Pahlow and Prowe, 2010). The low number of tuning parameters and the consequent rigidity of our model have facilitated the identification of the missing bidirectional trophic link in the original model. Thus, trade-off

and optimality-based models may constitute a promising avenue to reach a new level of (zooplankton) ecological modelling.

5. Acknowledgements

This work is funded by the German Research Foundation (DFG) as part of the Priority Programme 1704 (DynaTrait), and Sonderforschungsbereich 754 "Climate-Biogeochemistry Interaction in the Tropical Ocean" (www.sfb754.de). We thank H. Hauss and J. Franz for providing original data and helpful details of the mesocosm experiments. The help from Alexandra Marki in understanding the model performance is highly appreciated. We also thank the editor and two anonymous reviewers whose comments helped to improve the manuscript.

Appendix A.

Figs. A.1 and A.2 show the results of sensitivity simulations to investigate the effect of variable microzooplankton stoichiometry. Increasing the zooplankton N:P ratio by lowering the P:C ratio slightly improves the match between model and observations in the PU1 and PU2 mesocosm experiments.

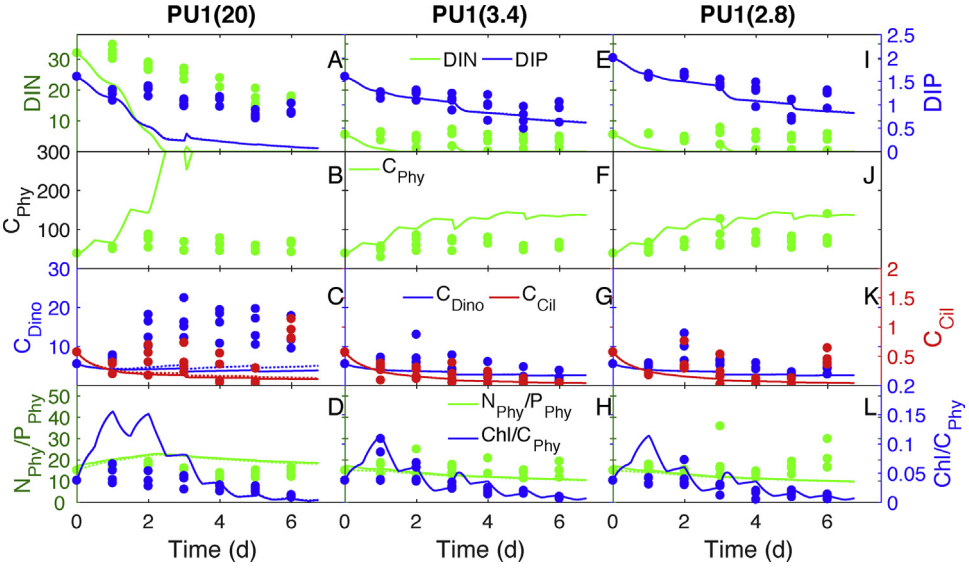

Fig. A.1. Same as Fig. 2, but with a lower P quota (P:C ratio) for microzooplankton (dinoflagellates and ciliates). Dotted lines show results with a lower P:C ratio in the NNPDrC configuration. Solid lines are the same as in Fig. 2.

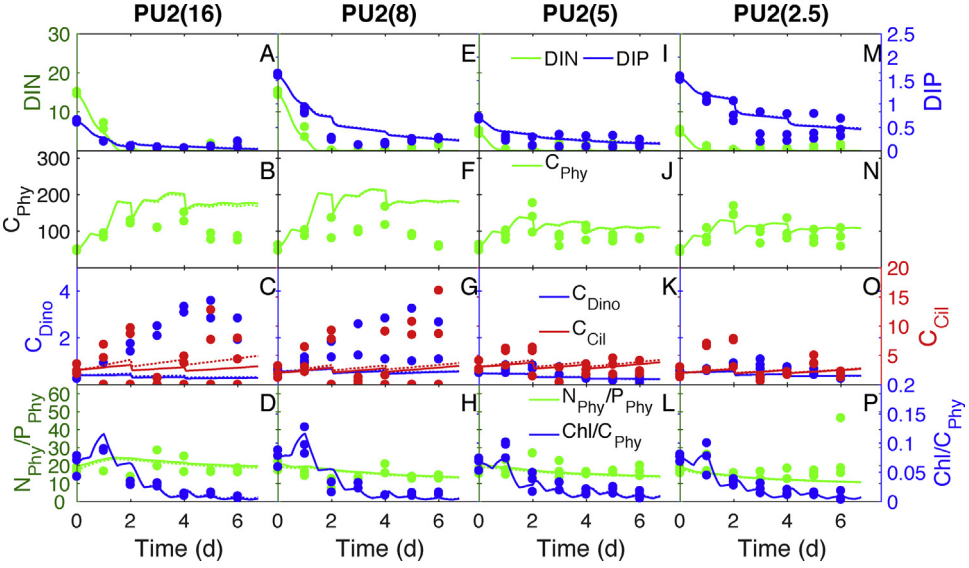

Fig. A.2. Same as Fig. 3, but with a lower P quota (P:C) for microzooplankton (dinoflagellates and ciliates). Dotted lines show results with a lower P:C ratio in the NNPDrC configuration. Solid lines are the same as in Fig. 3.

Appendix B. Supplementary data

A supplement which includes all equations describing the model is submitted together with the manuscript.

Supplementary data associated with this article can be found, in the online version, at https://doi.org/10.1016/j.ecolmodel.2017.11.013.

References

Acevedo-Trejos, E., Brandt, G., Smith, S.L., Merico, A., 2016. PhytoSFDM version 1.0.0: phytoplankton size and functional diversity model. Geosci. Model Dev. 9 (11), 4071–4085.

Ågren, G.I., 2004. The C:N:P stoichiometry of autotrophs – theory and observations. Ecol. Lett. 7, 185–191.

Andersen, K.H., Berge, T., Gonçalves, R., Hartvig, M., Heuschele, J., Hylander, S., Jacobsen, N.S., Lindemann, C., Martens, E.A., Neuheimer, A.B., et al., 2016. Characteristic sizes of life in the oceans, from bacteria to whales. Annu. Rev. Mar. Sci. 8, 217–241.

Aumont, O., Ethé, C., Tagliabue, A., Bopp, L., Gehlen, M., 2015. PISCES-v2: an ocean biogeochemical model for carbon and ecosystem studies. Geosci. Model Dev. 8, 2465–2513.

Banas, N.S., 2011. Adding complex trophic interactions to a size-spectral plankton model: emergent diversity patterns and limits on predictability. Ecol. Model. 222 (15), 2663–2675.

Barlow, R.G., Cummings, D.G., Gibb, S.W., 1997. Improved resolution of mono- and divinyl chlorophylls a and b and zeaxanthin and lutein in phytoplankton extracts using reverse phase C-8 HPLC. Mar. Ecol. Prog. Ser. 161, 303–307.

Brock, T.D., 1981. Calculating solar radiation for ecological studies. Ecol. Model. 14, 1–19.

Byrd, R.H., Gilbert, J.C., Nocedal, J., 2010. A trust region method based on interior point techniques for nonlinear programming. Math. Prog. 89, 149–185.

Chakraborty, S., Nielsen, L.T., Andersen, K.H., 2017. Trophic strategies of unicellular plankton. Am. Nat. 189 (4), 1–14.

Cropp, R., Moroz, I., Norbury, J., 2017. The role of grazer predation strategies in the dynamics of consumer-resource based ecological models. J. Sea Res. 125, 34–46.

Cropp, R., Norbury, J., 2012. The mechanisms of coexistence and competitive exclusion in complex plankton ecosystem models. Ecosystems 15, 200–212.

D'Alelio, D., Libralato, S., Wyatt, T., d'Alcala, M.R., 2016. Ecological-network models link diversity, structure and function in the plankton food-web. Sci. Rep. 6 (21806), 1–13.

Deutsch, C., Sarmiento, J.L., Sigman, D.M., 2007. Spatial coupling of nitrogen inputs and losses in the ocean. Nature 445, 163–167.

Dolan, J., 1992. Mixtrophy in ciliates: a review of chlorella symbiosis and chloroplast retention. Mar. Microb. Food Webs 6 (2), 115–132.

Dolan, J.R., Coats, D.W., 1991. A study of feeding in predacious ciliates using prey ciliates labeled with fluorescent microspheres. J. Plankton Res. 13 (3), 609–627.

Sterner, R.W., Elser, J.J., 2002. Ecological Stoichiometry: The Biology of Elements from Molecules to the Biosphere, 1st ed. Princeton University Press.

Evans, G.T., 2003. Defining misfit between biogeochemical models and data sets. J. Mar. Syst. 40-41, 49–54.

Flynn, K.J., Mitra, A., 2009. Building the "perfect beast": modelling mixotrophic plankton. J. Plankton Res. 31 (9), 965–992.

Flynn, K.J., Stoecker, D.K., Mitra, A., Raven, J.A., Glibert, P.M., Hansen, P.J., Granéli, E., Burkholder, J.M., 2013. Misuse of the phytoplankton-zooplankton dichotomy: the need to assign organisms as mixotrophs within plankton functional types. J. Plankton Res. 35 (1), 3–11.

Follows, M.J., Dutkiewicz, S., Grant, S., Chisholm, S.W., 2007. Emergent biogeography of microbial communities in a model ocean. Science 315, 1843–1846.

Franks, P.J., 2009. Planktonic ecosystem models: perplexing parameterizations and a failure to fail. J. Plankton Res. 31 (11), 1299–1306.

Franz, J., Krahmann, G., Lavik, G., Grasse, P., Dittmar, T., Riebesell, U., 2012a. Dynamics and stoichiometry of nutrients and phytoplankton in waters influenced by the oxygen minimum zone in the eastern tropical Pacific. Deep-Sea Res. I 62, 20–31.

Franz, J.M.S., Hauss, H., Sommer, U., Dittmar, T., Riebesell, U., 2012b. Production, partitioning and stoichiometry of organic matter under variable nutrient supply during mesocosm experiments in the tropical Pacific and Atlantic Ocean. Biogeosciences 9, 4629–4643.

Franzé, G., Modigh, M., 2013. Experimental evidence for internal predation in microzooplankton communities. Mar. Biol. 160, 3103–3112.

Fulton, E.A., Smith, A.D.M., Johnson, C.R., 2003a. Mortality and predation in ecosystem models: is it important how these are expressed? Ecol. Model. 169, 157–178.

Fulton, E.A., Smith, A.D.M., Johnson, C.R., 2003b. Effect of complexity on marine ecosystem models. Mar. Ecol. Prog. Ser. 253, 1–16.

Håkanson, L., 1995. Optimal size of predictive models. Ecol. Model. 78, 195–204.

Hansen, B., Bjornsen, P.K., Hansen, P.J., 1994. The size ratio between planktonic predators and their prey. Limnol. Oceanogr. 39, 395–403.

Hansen, H., Koroleff, F., 1999. Determination of nutrients. In: Grasshoff, K., Kremling, K., Ehrhardt, M. (Eds.), Methods of Seawater Analysis. , 3rd ed. Wiley-VCH Verlag GmbH, Weinheim, Germany, pp. 159–228 (Ch. 10).

Hansen, P.J., 1991. *Dinophysis* - a planktonic dinoflagellate genus which can act both as a prey and a predator of a ciliate. Mar. Ecol. Prog. Ser. 69, 201–204.

Hansen, P.J., Ojamäe, K., Berge, T., Trampe, E.C., Nielsen, L.T., Lips, I., Kühl, M., 2016. Photoregulation in a kleptochloroplastidic dinoflagellate, *Dinophysis acuta*. Front. Microbiol. 7 (785), 1–11.

Hauss, H., Franz, J.M., Sommer, U., 2012. Changes in N:P stoichiometry influence taxonomic composition and nutritional quality of phytoplankton in the Peruvian upwelling. Deep-Sea Res. 73, 74–85.

Hillebrand, H., Dürselen, C.-D., Kirschtel, D., Pollingher, U., Zohary, T., 1999. Biovolume calculation for pelagic and benthic microalgae. J. Phycol. 35, 403–424.

Jakobsen, H.H., Hansen, P.J., 1997. Prey size selection, grazing and growth response of the small heterotrophic dinoflagellate *Gymnodinium* sp. and the ciliate *Balanion comatum*-a comparative study. Mar. Ecol. Prog. Ser. 158, 75–86.

Jeong, H.J., Lim, A.S., Yoo, Y.D., Lee, M.J., Lee, K.H., Jang, T.Y., Lee, K., 2013. Feeding by heterotrophic dinoflagellates and ciliates on the free-living dinoflagellate *Symbiodinium* sp. (Clade E). Eukaryotic Microbiol. 61 (1), 27–41.

Jeong, H.J., Yoo, Y.D., Kim, J.S., Seong, K.A., Kang, N.S., Kim, T.H., 2010. Growth, feeding and ecological roles of the mixotrophic and heterotrophic dinoflagellates in marine planktonic food webs. Ocean Sci. 45 (2), 65–91.

Kalvelage, T., Lavik, G., Lam, P., Contreras, S., Arteaga, L., Löscher, C.R., Oschlies, A., Paulmier, A., Stramma, L., Kuypers, M.M.M., 2013. Nitrogen cycling driven by organic matter export in the South Pacific oxygen minimum zone. Nat. Geosci. 6, 228–234.

Kim, M., Nam, S.W., Shin, W., Coats, D.W., Park, M.G., 2012. *Dinophysis caudata* (Dinophyceae) sequesters and retains plastids from the mixotrophic ciliate prey *Mesodinium rubrum*. J. Phycol. 48, 569–579.

Kiørboe, T., 2013. Zooplankton body composition. Limnol. Oceanogr. 58 (5), 1843–1850.

Larsen, A., Egge, J.K., Nejstgaard, J.C., Di Capua, I., Thyrhaug, R., Bratbak, G., Thingstad, T.F., 2015. Contrasting response to nutrient manipulation in Arctic mesocosms are reproduced by a minimum microbial food web model. Limnol. Oceanogr. 60 (2), 360–374.

Le Quéré, C., Buitenhuis, E.T., Moriarty, R., Alvain, S., Aumont, O., Bopp, L., Chollet, S., Enright, C., Franklin, D.J., Geider, R.J., Harrison, S.P., Hirst, A.G., Larsen, S., Legendre, L., Platt, T., Prentice, I.C., Rivkin, R.B., Sailley, S., Sathyendranath, S., Stephens, N., Vogt, M., Vallina, S.M., 2016. Role of zooplankton dynamics for Southern Ocean phytoplankton biomass and global biogeochemical cycles. Biogeosciences 13 (14), 4111–4133.

Marki, A., Pahlow, M., 2016. Microzooplankton stoichiometric plasticity inferred from modeling mesocosm experiments in the Peruvian upwelling region. Front. Mar. Sci 3 (258), 1–15.

Menden-Deuer, S., Lessard, E.J., 2000. Carbon to volume relationships for dinoflagellates, diatoms, and other protist plankton. Limnol. Oceanogr. 45 (3), 569–579.

Mitra, A., Castellani, C., Gentleman, W.C., Jónasdóttir, S.H., Flynn, K.J., Bode, A., Halsband, C., Kuhn, P., Licandro, P., Agersted, M.D., Calbet, A., Lindeque, P.K., Koppelmann, R., Møller, E.F., Gislason, A., Nielsen, T.G., John, M.S., 2014a. Bridging the gap between marine biogeochemical and fisheries sciences; configuring the zooplankton link. Prog. Oceanogr. 129 (Part B), 176–199.

Mitra, A., Flynn, K.J., Burkholder, J.M., Berge, T., Calbet, A., Raven, J.A., Graneli, E., Glibert, P.M., Hansen, P.J., Stoecker, D.K., Thingstad, F., Tillmann, U., Vage, S., Wilken, S., Zubkov, M.V., 2014b. The role of mixotrophic protists in the biological carbon pump. Biogeosciences 11, 995–1005.

Mitra, A., Flynn, K.J., Tillmann, U., Raven, J.A., Caron, D., Stoecker, D.K., Not, F., Hansen, P.J., Hallegraeff, G., Sanders, R., Wilken, S., McManus, G., Johnson, M., Pitta, P., Vage, S., Berge, T., Calbet, A., Thingstad, F., Jeong, H.J., Burkholder, J., Glibert, P.M., Graneli, E., Lundgren, V., 2016. Defining planktonic protist functional groups on mechanisms for energy and nutrient acquisition: incorporation of diverse mixotrophic strategies. Protist 167, 106–120.

Montagnes, D., 2013. Ecophysiology and behavior of tintinnids. In: Dolan, J.R., Montagnes, D.J.S., Agatha, S., Coats, W.D., Stoecker, D.K. (Eds.), The Biology and Ecology of Tintinnid Ciliates: Models for Marine Plankton. John Wiley & Sons, The Atrium, Southern Gate, Chichester, West Sussex, PO19 8SQ, UK, pp. 85–121 (Ch. 4).

Nishitani, G., Nagai, S., Sakiyama, S., Kamiyama, T., 2008. Successful cultivation of the toxic dinoflagellate *Dinophysis caudata* (Dinophyceae). Plankton Benthos Res. 3 (2), 78–85.

Pahlow, M., Dietze, H., Oschlies, A., 2013. Optimality-based model of phytoplankton growth and diazotrophy. Mar. Ecol. Prog. Ser. 489, 1–16.

Pahlow, M., Prowe, A.E.F., 2010. Model of optimal current feeding in zooplankton. Mar. Ecol. Prog. Ser. 403, 129–144.

Pahlow, M., Vézina, A.F., Casault, B., Maass, H., Malloch, L., Wright, D.G., Lu, Y., 2008. Adaptive model of plankton dynamics for the North Atlantic. Prog. Oceanogr. 76, 151–191.

Park, M.G., Kim, M., Kim, S., Yih, W., 2010. Does *Dinophysis caudata* (Dinophyceae) have permanent plastids? J. Phycol. 46, 236–242.

Prowe, A.E.F., Pahlow, M., Dutkiewicz, S., Follows, M., Oschlies, A., 2012a. Top-down control of marine phytoplankton diversity in a global ecosystem model. Prog. Oceanogr. 101 (1), 1–13.

Prowe, A.E.F., Pahlow, M., Oschlies, A., 2012b. Controls on the diversity-productivity relationship in a marine ecosystem model. Ecol. Model. 225, 167–176.

Redfield, A.C., 1934. On the Proportions of Organic Derivations in Sea Water and Their Relation to the Composition of Plankton. University Press of Liverpool James Johnstone Memorial, pp. 177–192.
Sailley, S.F., Vogt, M., Doney, S.C., Aita, M.N., Bopp, L., Buitenhuis, E.T., Hashioka, T., Lima, I., Le Quéré, C., Yamanaka, Y., 2013. Comparing food web structures and dynamics across a suite of global marine ecosystem models. Ecol. Model. 261–262, 43–57.
Schartau, M., Wallhead, P., Hemmings, J., Löptien, U., Kriest, I., Krishna, S., Ward, B.A., Slawig, T., Oschlies, A., 2017. Reviews and syntheses: parameter identification in marine planktonic ecosystem modelling. Biogeosciences 14, 1647–1701.
Sharp, J.H., 1974. Improved analysis for "particulate" organic carbon and nitrogen from seawater. Limnol. Oceanogr. 6, 984–989.
Sherr, E.B., Sherr, B.F., 1987. High rates of consumption of bacteria by pelagic ciliates. Nature 325, 710–711.
Stoecker, D.K., 2012. Predators of tintinnids. In: Dolan, J.R., Montagnes, D.J.S., Agatha, S., Coats, D.W., Stoecker, D.K. (Eds.), The Biology and Ecology of Tintinnid Ciliates: Models for Marine Planktonnd Ecology of Tintinnid Ciliates: Models for Marine Plankton. John Wiley & Sons, Ltd., pp. 122–144 (Ch. 5).
Stoecker, D.K., Hansen, P.J., Caron, D.A., Mitra, A., 2017. Mixotrophy in the marine plankton. Annu. Rev. Mar. Sci. 9, 311–335.
Strom, S.L., 1991. Growth and grazing rates of the herbivorous dinoflagellate *Gymnodinium* sp. from the open subarctic Pacific Ocean. Mar. Ecol. Prog. Ser. 78, 103–113.
Su, B., Pahlow, M., Wagner, H., Oschlies, A., 2015. What prevents nitrogen depletion in the oxygen minimum zone of the eastern tropical South Pacific? Biogeosciences 12, 1113–1130.
Thingstad, T.F., Havskum, H., Zweifel, U.L., Berdalet, E., Sala, M.M., Peters, F., Alcaraz, M., Scharek, R., Perez, M., Jacquet, S., et al., 2007. Ability of a "minimum" microbial food web model to reproduce response patterns observed in mesocosms manipulated with N and P, glucose, and Si. J. Mar. Syst. 64 (1), 15–34.
Vallina, S., Ward, B.A., Dutkiewicz, S., Follows, M.J., 2014. Maximal feeding with active prey-switching: a kill-the-winner functional response and its effect on global diversity and biogeography. Prog. Oceanogr. 120, 93–109.
Walve, J., Larsson, U., 1999. Carbon, nitrogen and phosphorus stoichiometry of crustacean zooplankton in the Baltic Sea: implications for nutrient recycling. J. Plankton Res. 21 (12), 2309–2321.
Ward, B.A., Dutkiewicz, S., Barton, A.D., Follows, M.J., 2011. Biophysical aspects of resource acquisition and competition in algal mixotrophs. Am. Nat. 178 (1), 98–112.
Ward, B.A., Dutkiewicz, S., Follows, M.J., 2014. Modelling spatial and temporal patterns in size-structured marine plankton communities: top-down and bottom-up controls. J. Plankton Res. 36, 31–47.
Wirtz, K.W., 2012. Who is eating whom? Morphology and feeding type determine the size relation between planktonic predators and their ideal prey. Mar. Ecol. Prog. Ser. 445, 1–12.
Wirtz, K.W., 2013. Mechanistic origins of variability in phytoplankton dynamics. Part I: niche formation revealed by a size-based model. Mar. Biol. 160 (9), 2319–2335.
Yasindi, A.W., Taylor, W.D., 2006. The trophic position of planktonic ciliate populations in the food webs of some East African lakes. Afr. J. Aquat. Sci. 31 (1), 53–62.